C+L-Band 16 × 16 16-Channel Silicon Photonics Wavelength Cross-Connect Switch Based on Waveguide Bragg Gratings

Kazuhiro Ikeda, Ryotaro Konoike, Keijiro Suzuki

Platform Photonics Research Center, National Institute of Advanced Industrial Science and Technology, 305-8568, Tsukuba, Japan, kaz.ikeda@aist.go.jp

Abstract *We demonstrate a largest ever port- and channel-count monolithically integrated wavelength cross-connect switch using 256 FSR-free grating-assisted contra-directional couplers and 1,024 thermo-optic Mach-Zehnder switches. The fabricated chip was fully packaged and controlled to measure spectra of representative switching states for all the 16 wavelength channels.*

Introduction

Wavelength selective switches (WSSs) and wavelength cross-connects (WXCs) play an important role in flexible optical networking and have been deployed in the reconfigurable optical add-drop multiplexing (ROADM) systems for telecom networks [1]. Recent rapid growth of information traffic in datacentre networks attracts increasing attention to the use of a high degree of wavelength division multiplexing (WDM) and therefore WSSs and WXCs in future datacentres [2]. Silicon photonics offers highly integrated ultra-small devices with low power consumption as well as fast switching speed [3], which are desirable features in datacentres and computing platforms, and therefore a number of silicon photonics WSSs have been reported using ring resonators [4], arrayed waveguide gratings (AWGs) [5], and echelle gratings [6]. We have proposed and demonstrated a new type of silicon photonics WXC switch using Mach-Zehnder interferometers (MZIs) and contra-directional couplers (C-DCs) [7,8]. The silicon photonics C-DCs consist of two coupled waveguides with sidewall corrugation that induces mode coupling between the waveguides in the counter direction at a Bragg wavelength [9]. Due to the first order operation, the C-DC has practically an unlimited free spectral range (FSR) and is suitable for multiband add-drop filters. In addition, the large index modulation of the silicon waveguide corrugation induces a large coupling coefficient leading to a wide and flattop spectral shape, which offers high tolerance for temperature change and is suited for cost effective coarse WDM systems.

In this paper, we extend our proposed device architecture and demonstrate the largest ever scale monolithically integrated WXC with 16 × 16 ports and 16 wavelength channels (the largest so far was 8 × 8 ports and 8 wavelength channels [6]). The WXC consists of 256 FSR-free grating-assisted C-DCs and 1,024 thermo-optic (TO) MZIs, integrated on a 11 mm × 26 mm silicon chip. The fabricated chip is fully packaged and controlled to measure spectra of representative switching states for all the 16 wavelength channels over the C+L band.

Design and Fabrication

Figure 1(a) shows a schematic of a single C-DC where structure parameters are defined. In this study, we used W_1 = 350 nm, W_2 = 450 nm, ΔW_1 = 30 ~ 40 nm, ΔW_2 = 50 ~ 60 nm, Λ = 352 ~ 388 nm, L ~ 800 μm, and G = 250 nm. The grating modulation widths, ΔW_1 and ΔW_2, were varied for each wavelength channel to equalize the width of the stopband. Also, the grating modulation widths were Gaussian-apodized.

Figure 1(b) describes a schematic diagram of a 16 × 16 switch used for the WXC, which consists of 8 × 8 = 64 MZIs (2 × 2 TO switches) and waveguide intersections in between. Note that this usage of the 8 × 8 matrix of MZIs as a 16 × 16 switch results in a blocking switch. In another usage, we can obtain two synchronous sets of 8 × 8 strictly non-blocking switch (path-independent insertion loss (PILOSS) switch) with a specific port assignment [3].

Figure 1(c) explains the configuration and operation of our 16 × 16 16-ch silicon photonics WXC using the C-DCs and 16 × 16 switches described in Figs. 1(a) and 1(b). 16 C-DCs for different wavelength channels are cascaded, and each drop port is connected to each of the 16 × 16 switches designed for the corresponding wavelengths (MZIs are optimized for designated wavelengths). The cascaded C-DCs are parallelly placed for each of the 16 waveguide ports, also connecting to each 16 × 16 switch. An example wavelength routing is also shown with coloured arrows in Fig. 1(c), where 4 wavelength channels are introduced to input port 1 and demultiplexed to output ports 1, 2, 15, and 16. The region surrounded by the dotted square functions as a 16 × 16 switch for a single wavelength but does nothing for the other wavelengths.

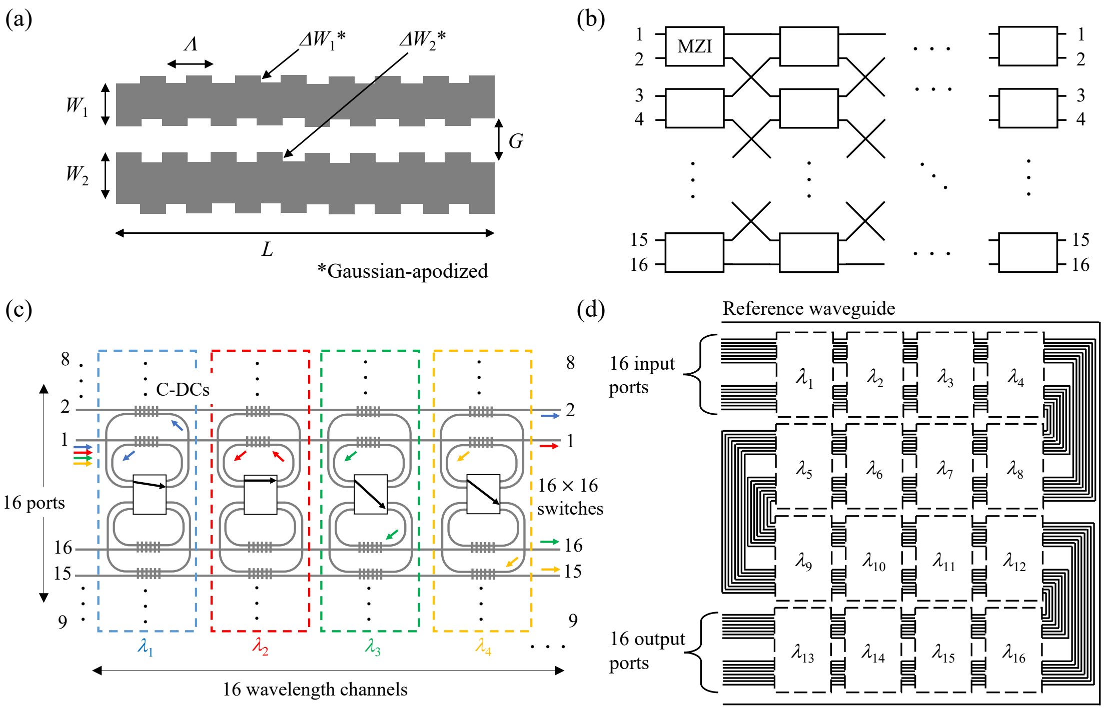

Fig. 1: Schematic diagrams of (a) C-DC, (b) 16 × 16 MZI-based switch, and (c) 16 × 16 16-ch silicon photonics WXC with an example wavelength routing (4 wavelength channels at input 1 demultiplexed to output 1, 2, 15, 16). (d) Circuit layout of the switch chip.

We laid out the 16 × 16 16-ch silicon photonics WXC circuit as schematically depicted in Fig. 1(d) so that the overall circuit is densely packed. All the input and output ports were placed on one side of the chip with a pitch of 250 μm, including a reference waveguide surrounding the whole circuit for fibre array alignment and estimation of the fibre-to-chip coupling loss. TE-pass polarizers were integrated into all the input and output ports to suppress the TM light since the WXC is designed for the TE mode.

The 16 × 16 16-ch silicon photonics WXC chip was fabricated using our 300-mm CMOS R&D foundry with 45-nm ArF immersion lithography [3]. Fig. 2(a) shows a micrograph of the 11 mm × 26 mm chip diced from the processed 300-mm wafer, on which 256 C-DCs (16 ports × 16 wavelengths) and 1,024 MZIs (2,048 microheaters) (64 (128) × 16) were integrated. A magnified view of a 16 × 16 switch for a single wavelength channel surrounded by the white square is shown in Fig. 2(b) where an SEM image of a C-DC taken during the fabrication process is also shown in the inset. Note that a waveguide intersection was placed after each MZI to exchange the bar and the cross ports. This can improve the leakage at the bar port of the 2 × 2 switch which is useful when operated as two synchronous PILOSS switches [3]. The WXC chip with more than 2,000 electrical pads was first flip-chip bonded to a ceramic interposer to extend the pad arrangement to a 0.5-mm land grid array, then attached by a 34-port high-NA fibre array with a MFD of ~ 4 μm. The assembled device was inserted into the socket on the control circuit board as shown in Fig. 2(c). As detailed in ref. [3], the switching time of the WXC is expected to be less than 5 μs.

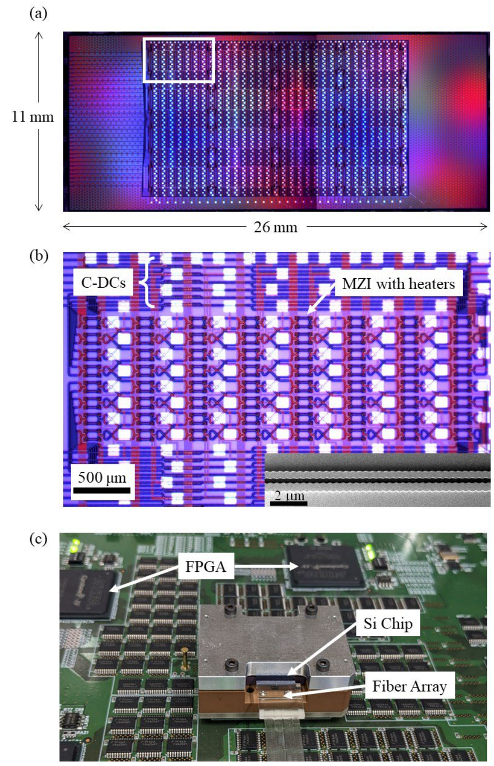

Fig. 2: Photographs of (a) fabricated switch chip, (b) single wavelength region on the chip indicated by the white square in (a) (Inset: SEM image of C-DC), and (c) control circuit board mounted with assembled WXC and FPGAs.

Characterization

Firstly, a C + L band ASE light source polarized to the TE polarization of the device was introduced to the input port 8 of the WXC. We routed one of the 16 wavelength channels to output port 9 (8-to-9) while the other channels were set to the 8-to-8 connection. We repeated this for the 16 channels and measured the transmission spectra from the output port 8 (through) and 9 (drop) using an optical spectrum analyser, as shown in Fig. 3(a) and 3(b) respectively. Also shown in Fig. 3(c) is transmission spectra from the output port 8 and 9 for another example switching state, where channels 1, 4, 7, 10, 13, and 16 were, at the same time, set to the 8-to-9 connection while the other channels were set to the 8-to-8 connection. We can see that the 16 channels are distributed over a wide wavelength range of the C and L bands. The bandwidth of the wavelength channels is around 4 nm. Note that the channels 3, 8, and 11 that are overlapped with the adjacent ones have narrower bandwidths in Fig. 3(b) because the overlapped spectral component routed to port 9 is again routed to some other port by the adjacent C-DC and switch. The transmission spectrum of the reference waveguide was also measured and plotted in the figures. The fibre-to-fibre transmission of the reference waveguide is −11.5 dB at 1550 nm, from which the fibre-to-chip coupling loss is estimated as 3.1 dB/facet by subtracting the loss of the waveguide. A loss difference between the reference waveguide and the signal paths at around 1585 nm (outside any of the C-DC bands) is ~6 dB, from which we estimate a loss of the single C-DC to be ~0.18 dB by (6 – 3.2 (waveguide length increase)) / 16. A loss increase at a C-DC centre wavelength from the loss at ~1585 nm is ~3.5 dB which corresponds to a loss of the 16 × 16 MZI-based switch. An on-chip loss of the WXC is then estimated to be 11.5 + 6 + 3.5 – 6.2 = 14.8 dB.

Secondly, the ASE light was introduced to the input port 9. The wavelength channels 1, 2, 3…, were routed to the output port 1, 2, 3…, and then switched to the output port 16, 15, 14…, respectively. The measured spectra from all the 16 output ports at the 2 switch states are shown in Fig. 4. We can see successful switching while some peaks outside each channel band. These spectral components originate from the spectral overlaps between adjacent channels explained above, and therefore are off the channel wavelengths indicated by the dotted vertical lines and do not become crosstalk.

Conclusion

We have demonstrated a C+L-Band 16 × 16 16-ch silicon photonics WXC based on C-DCs and MZIs. Since the operation bandwidth of this WXC is not limited by FSR, a design for further broadband operation is possible, which will be useful for future multiband network systems.

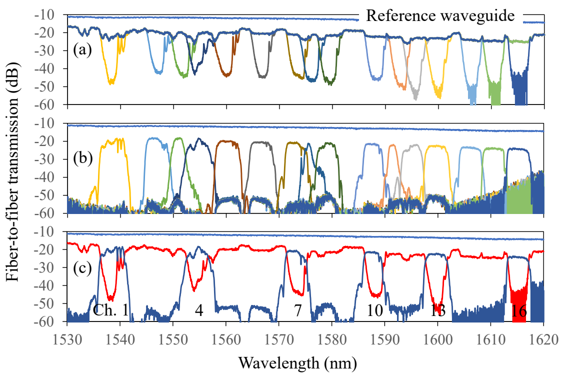

Fig. 3: Measured spectra from (a) output port 8 and (b) 9 when each of 16 wavelength channels was set to 8-to-9, (c) output 8 and 9 when selected channels were set to 8-to-9. The other channels were set to 8-to-8 in all cases.

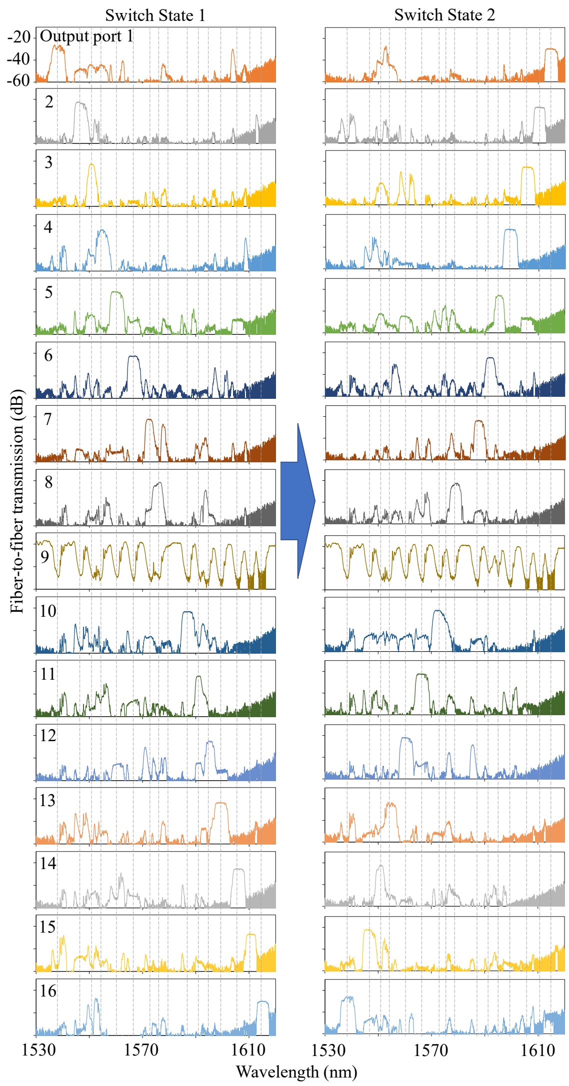

Fig. 4: Measured spectra from all 16 output ports for 2 switch states where wavelength channels 1, 2, 3… were set to 9-to-1, 2, 3… and 9-to-16, 15, 14…, respectively. Vertical dotted lines indicate the channel wavelengths.

References

[1] T. A. Strasser and J. L. Wagener, "Wavelength-selective switches for ROADM applications", IEEE Journal of Selected Topics on Quantum Electronics., vol. 16, no. 5, pp. 1150-1157, 2010, DOI: 10.1109/JSTQE.2010.2049345.

[2] Q. Cheng, S. Rumley, M. Bahadori and K. Bergman, "Photonic switching in high performance datacenters [Invited]", Optics Express, vol. 26, pp. 16022-16043, 2018, DOI: 10.1364/OE.26.016022

[3] K. Ikeda, K. Suzuki, R. Konoike, S. Namiki, and H. Kawashima, "Large-scale silicon photonics switch based on 45-nm CMOS technology," Optics Communications, vol. 466, p. 125677, 2020, DOI: 10.1016/j.optcom.2020.125677

[4] A. S. P. Khope, M. Saeidi, R. Yu, X. Wu, A. M. Netherton, Y. Liu, Z. Zhang, Y. Xia, G. Fleeman, A. Spott, S. Pinna, C. Schow, R. Helkey, L. Theogarajan, R. C. Alferness, A. A. M. Saleh, and J. E. Bowers, "Multi-wavelength selective crossbar switch," Optics Express, vol. 27, pp. 5203–5216, 2019. DOI: 10.1364/OE.27.005203

[5] F. Nakamura, K. Muramatsu, K. Suzuki, K. Tanizawa, M. Ohtsuka, N. Yokoyama, K. Matsumaro, M. Seki, K. Koshino, K. Ikeda, S. Namiki, H. Kawashima, and H. Tsuda, "Integrated silicon photonic wavelength-selective switch using wavefront control waveguides," Optics Express, vol. 26, pp. 13573–13589, 2018, DOI: 10.1364/OE.26.013573

[6] T. J. Seok, J. Luo, Z. Huang, K. Kwon, J. Henriksson, J. Jacobs, L. Ochikubo, R. S. Muller, and M. C. Wu, "Silicon photonic wavelength cross-connect with integrated MEMS switching," APL Photonics, vol. 4, 100803, 2019. DOI: 10.1063/1.5120063

[7] K. Ikeda, K. Suzuki, R. Konoike, and H. Kawashima, "Silicon Photonics Wavelength Selective Switch with Unlimited Free Spectral Range," Journal of Lightwave Technology, vol. 38, pp. 3268–3272, 2020, DOI: 10.1109/JLT.2020.2989379

[8] K. Ikeda, R. Konoike, K. Suzuki, H. Kawashima, "2 × 2 16-ch silicon photonics wavelength-selective switch based on waveguide gratings," Optics Express, vol. 28, pp. 26861-26869, 2020, DOI: 10.1364/OE.402546

[9] K. Ikeda, M. Nezhad, and Y. Fainman, "Wavelength selective coupler with vertical gratings on silicon chip," Applied Physics Letters, vol. 92, 201111, 2008, DOI: 10.1063/1.2936862